

# Moving from a 3D Axial Flux Machine Model to 2D Considering the Impact of End Leakage Flux

Downloaded from: https://research.chalmers.se, 2025-11-16 23:05 UTC

Citation for the original published paper (version of record):

Puttaraj, V., Lundmark, S., Thiringer, T. (2024). Moving from a 3D Axial Flux Machine Model to 2D Considering the Impact of End Leakage Flux. 2024 International Conference on Electrical Machines, ICEM 2024. http://dx.doi.org/10.1109/ICEM60801.2024.10700366

N.B. When citing this work, cite the original published paper.

research.chalmers.se offers the possibility of retrieving research publications produced at Chalmers University of Technology. It covers all kind of research output: articles, dissertations, conference papers, reports etc. since 2004. research.chalmers.se is administrated and maintained by Chalmers Library

# Moving from a 3D Axial Flux Machine Model to 2D Considering the Impact of End Leakage Flux

#### Vineetha Puttaraj

Department of Electrical Engineering Chalmers University of Technology Gothenburg, Sweden vineetha@chalmers.se or (i)

#### Sonja Tidblad Lundmark

Department of Electrical Engineering Chalmers University of Technology Gothenburg, Sweden sonja.lundmark@chalmers.se or (D)

#### Torbjörn Thiringer

Department of Electrical Engineering Chalmers University of Technology Gothenburg, Sweden

torbjorn.thiringer@chalmers.se or (D)



Abstract—Axial Flux Machines (AFMs) may have a potential of smaller axial length and higher power and torque density compared to the Radial Flux Machines (RFMs). However, the AFM needs to be modeled in Three-Dimensions (3D) yielding a large computation time when solving the Finite Element Method (FEM) model. A larger extent of computation time can be reduced by transforming the 3D problem to a Two-Dimensional (2D) problem. A single computation plane located at the center of the magnet in the 3D model is employed. This transformation leads to a loss of information due to the leakage flux in the axial direction, mainly around the rotor magnets and around the stator end windings. The purpose of this paper is to transform the 3D AFM model to a 2D model and quantify the consequences. An off-the-shelf outer stator inner rotor reference AFM is compared with an equivalent 3D FEM model. Several 3D and 2D models with varying core and magnet lengths were compared. A model with narrow core and magnet lengths was further investigated for five different model sizes ranging from full 3D to 2D. The results for the investigated machine type reveal that the rotor magnet leakage contributes to a dominant effect that necessitates a 3D model if a magnetically leading rotor core surrounds the magnet in the radial direction, and when the radial thickness of the magnets is small. Similarly, winding end leakage effects must be modeled in 3D when the radial thickness of the stator core is small relative to the coil end extent.

Index Terms-Axial flux permanent magnet machine, Finite element method modeling, 3D to 2D transformation

#### I. INTRODUCTION

**T**N the era of Electric Vehicle (EV) technology, Axial Flux Permanent Magnet (AFPM) machines have gained significance for their attractive features of having higher power and torque densities. The smaller axial length of Axial Flux Machines (AFMs) results in a flattened machine structure in comparison to the Radial Flux Machines (RFMs) [1] and [2].

The AFM is a Three-Dimensions (3D) problem with flux paths in all three directions (axial, radial, and circumferential). Transforming a 3D FEM model to a 2D FEM model saves computation time. In [3], the Axial Flux Permanent Magnet Synchronous Machine (AFPMSM) is transformed into smaller pieces of 3D models, and each piece is transformed to an equivalent 2D model and the average values of these models are computed. Various design variations like magnet segmentation [4], an end effect due to flux leakage in magnetic gears

The authors gratefully acknowledge the financial support provided by the Swedish Electromobility Center and Chalmersska Forskningsfonden.

[5] are studied in the literature. The geometrical shape of the core in an AFM cannot be radially proportional due to manufacturing requirements [6]. In [7], the author demonstrates the 2D Linear Motor Modelling Approach (2D-LMMA), with other model transformation techniques and concludes that 2D-LMMA is best suited. In some special cases with no central symmetry in the magnet structure like skewed magnets, it is preferable to have more number of segments using the model transformation approaches. These transformation approaches are also extended in [8] to model an axial flux induction machine to the 2D equivalent, resulting in acceptable error rates with certain resizing of the machine tooth thickness and stator structures.

In [9], the 2D-LMMA approach is used to optimize the torque output and demonstrates that the 2D model can be a base for conducting optimization. In [10], the 3D model is transformed to an equivalent 2D linear model, and the output performance of these two models are made equal by selecting the same volume and operating point of the magnetic material. In [11], a new methodology of combining the 2D model and analytical calculation is presented to have a better accuracy as compared to a 2D approximation model of an AFM.

The purpose of this paper is to investigate the leakage flux around the magnets and the end winding of the 3D FEM model of an AFM and the corresponding 2D representation of the AFM with a single computational plane. A 4kW offthe-shelf reference AFPM machine is bench-marked and an equivalent 3D FEM model of the reference machine is created. The 3D model is transformed to a 2D model using the 2D-LMMA approach. Several 3D and 2D models were created with varying core and magnet lengths. Further, these models were compared and the models yielding higher differences in the magnitude of the flux linkages were investigated and analyzed.

#### II. MODELLING OF AXIAL FLUX PERMANENT MAGNET (AFPM) MACHINE IN 3D AND 2D

#### A. Description of the reference Axial Flux Machine

The off-the-shelf reference AFM is an inner rotor outer stators machine type with inset permanent magnets as shown in Fig.1. The two stator windings are connected in parallel. The machine's dimensions were extracted from dismantled pieces of the reference machine. The stator lamination is rolled in the radial direction. The air gap in the axial direction as well as the material data of the stator core, rotor core, and magnets are unknown. The machine data is given in Table I.

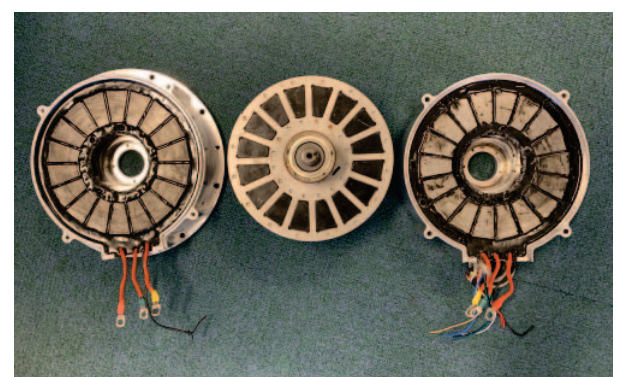


Fig. 1. Reference AFPM machine

TABLE I REFERENCE AFPM MACHINE DATA

Description	Value		
General details			
Rated power	$4 \ kW$		
Peak power	8~kW		
Rated speed	$2000 \ rpm$		
Maximum speed	$4000 \ rpm$		
Rated torque	19 Nm		
Peak Torque	50 Nm		
Number of poles	16		
Number of slots	18		
Type of cooling	Natural air cooling		
Dimension details of reference machi	Dimension details of reference machine and 3D model		
Outer diameter of stator core	166.2 mm		
Inner diameter of stator core	$94.2 \ mm$		
Outer diameter of rotor core	$186.2 \ mm$		
Inner diameter of rotor core	38 mm		
Length of magnet in radial direction, $L_m$	34 mm		
Length of tooth in radial direction	36 mm		
Stator core length in positive z-direction	$30 \ mm$		
Rotor core and magnet length in z-direction	7 <i>mm</i>		
Winding details			
Diameter of single copper strand	$0.88 \ mm$		
Number of winding layers	2		
Number of turns	10		
Number of parallel branches	1		
Type of winding	Concentrated		

#### B. FEM Modelling of the Reference AFPM machine

The electromagnetic field problems are solved using Maxwell's equations in a finite region of space with appropriate boundary conditions. The model is built in the Ansys Maxwell software. The dimensions and other FEM model details are provided in Table I and II respectively. The built 3D FEM model is shown in Fig.2 representing the full-size model and Fig.3 representing one-quarter of the full-size model and the necessary boundary conditions.

#### C. Transforming the 3D model to a 2D model

The 3D FEM model is transformed to a 2D model using the 2D-LMMA approach. The computational plane is located along the average radius of the outer and inner radius of the

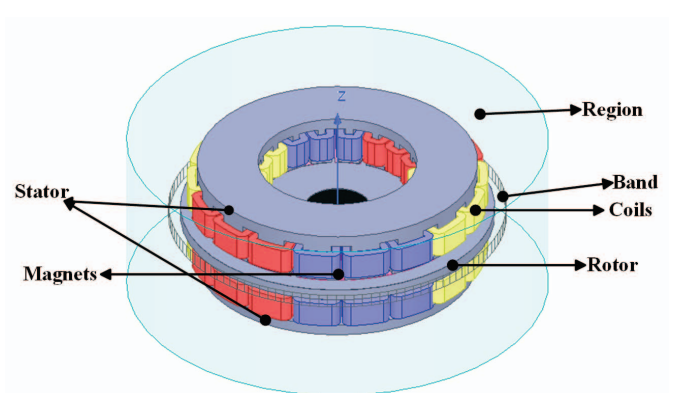


Fig. 2. 3D FEM model of reference AFPM machine

TABLE II 3D AFPM MACHINE FEM MODEL DATA

Description	Value
Boundary type	Matching and symmetry
Core material	SURA M235-35A
Magnet material	NdFeB-33UH and NdFeB-28ah
Symmetry multiplier	2
Number of time steps	120

magnet in the 3D model,  $R_{wp}$ . The process of transformation from a 3D model to a 2D model is demonstrated in Fig. 4.

#### D. Motivation for transforming a 3D model to a 2D model

The cross-section area along the XY and XZ plane of the 3D FEM models are compared with the equivalent 2D model, tabulated in Table.III. From Table III it is evident that the cross-section areas of the 3D and 2D models are the same in most cases. Despite having almost the same cross-section area, the 3D model needs much longer computation time, and more mesh elements as seen in Table IV. The longer computation time in the 3D model is the key motivating factor paving the way for transforming the 3D model to a 2D model.

## III. COMPARISON OF REFERENCE AFPM MACHINE WITH 3D AND 2D FEM MODELS

In this section, the off-the-shelf reference AFPM machine is compared with its equivalent 3D and 2D FEM model.

The no-load induced voltage of the reference AFPM machine and its equivalent 3D FEM model with the transformed 2D model are compared when the reference machine was operated at 500 rpm.

The measured no-load induced voltage of the reference AFPM machine with 500rpm was used to derive no-load flux

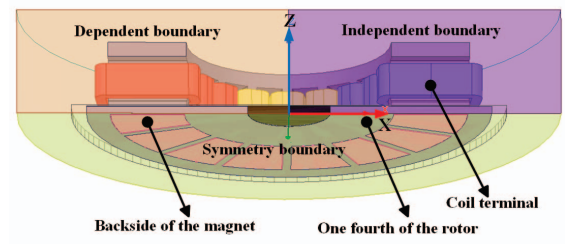


Fig. 3. Symmetrical piece of the full model with assigned boundary condition. Purple rectangle - independent boundary; Orange rectangle - dependent boundary; yellow semi-circle - symmetry boundary.

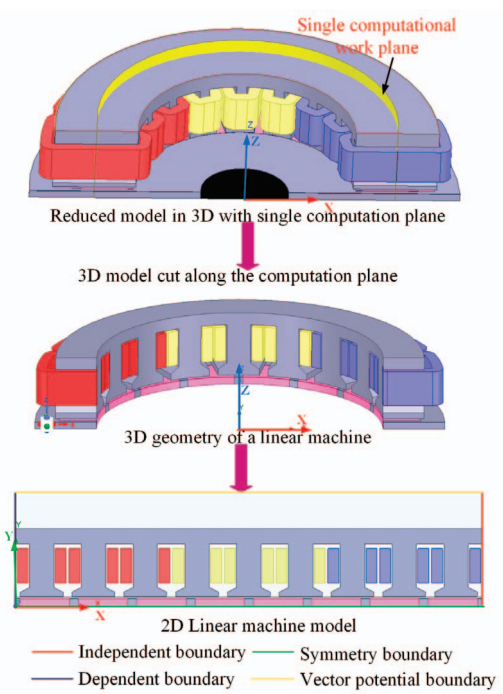


Fig. 4. Process of transforming a 3D model to a 2D model; yellow curved sheet is the computational plane used to form the 2D model.

TABLE III
COMPARISON OF CROSS-SECTION AREAS

Part of the motor	3D model	2D model		
Along XY plane for 3D model and along depth for 2D model				
Stator tooth body <sup>a</sup>	$385 \ mm^2$	$364 \ mm^2$		
Stator tooth rim <sup>a</sup>	$674 \ mm^2$	636 $mm^2$		
Single magnet	$733 \ mm^2$	733 $mm^2$		
Rotor core <sup>b</sup>	$7,180 \ mm^2$	$1,090 \ mm^2$		
Along XZ plane for 3D model and along XY plane for 2D model				
Stator cross-section	$3,840 \ mm^2$	$3,840mm^2$		
Coil cross-section	$73 \ mm^2$	$73 \ mm^2$		
Single magnet	$75 \ mm^2$	$75  mm^2$		
Rotor core	$112 \ mm^2$	$112 \ mm^2$		

a difference is due to the selection of depth = magnet length

linkage, which in turn was compared with the equivalent 3D and 2D models of the AFPM machine. The resulting flux linkage of the reference AFPM machine is plotted in Fig. 5a

The model geometry of magnets and coils differs slightly between the 3D and 2D models. The reference AFPM machine and the 3D FEM model have trapezoidal-shaped magnets and the 2D model has rectangular-shaped magnets. Furthermore, the end parts of the coils are not included in the 2D model. However, the comparison of the cross-section area in Table III shows that geometrically the cross-section areas are the same with a few exceptions. The 3D and 2D models are also compared at different magnet and core lengths in the radial direction. The comparison includes the magnetic flux linkage

 $\label{thm:constraint} TABLE\ IV \\ 3D\ \text{and}\ 2D\ \text{model}\ \text{mesh}\ \text{data}\ \text{and}\ \text{simulation}\ \text{time}\ \text{details}$ 

	3D model	2D model
Simulation time	16 hrs 15 min	05 min
Number of mesh elements	384,000	5,100

and its relative percentage difference along with the average torque, average core loss and magnet loss for both no load and rated conditions. These comparisons are illustrated in Fig.5.

In Fig. 5a showing flux linkages, a diamond-shaped marker indicates a percentage difference of less than 5% between the 3D model and the 2D model for a magnet length of 34mm. Conversely, a star-shaped marker signifies a higher percentage difference of 39% between the 3D and 2D models for a magnet length of 4mm.

The average torque and average core loss comparison are depicted in Fig. 5b and 5c. It is observed that the discrepancies between the 3D and 2D models for torque and core loss values at rated motor operation are small across various magnet and core lengths.

The complex three-dimensional nature of eddy current formation results in larger differences in average magnet losses between the 3D and 2D models under rated operation, as illustrated in Fig. 5d. The complex behavior of magnetic fields at the edges and corners of the magnets are not accurately accounted for in the 2D model hence this leads to simplified and less accurate magnetic field distributions. The leakage flux paths that extend outside the computational plane of the 2D model are not captured. Under the rated operating point, the leakage flux and the edge effects become more significant, leading to an inaccurate representation of the magnetic field around the magnets due to leakage flux and pronounced saturation near the edges of the magnets.

At the rated operating point, the uniform field distribution in the 2D model becomes less valid as different parts of the machine experience varying magnetic flux levels and saturation. This simplified assumption of uniform flux distribution in the 2D model can lead to an overestimation of eddy currents in the magnets, whereas, the 3D model captures the complexity of the magnetic field distribution, including edge effects, leakage flux paths, and non-uniformities, resulting in a more accurate representation of the magnetic environment within the magnets.

### IV. INVESTIGATION OF THE DIFFERENCES BETWEEN 3D AND THE 2D FEM AFPM MACHINE MODEL

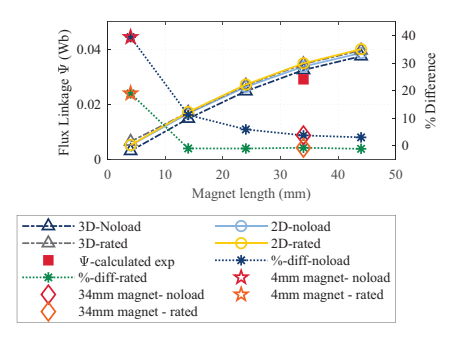
#### A. Investigated Machine Models

The model with the narrow core is selected to further investigate the limitations of reducing the model from a full 3D model. The model geometry of the 4mm core was altered in five ways, and leakage due to various parts was investigated. The modifications in model geometry are listed in Table V and illustrated in Fig. 6.

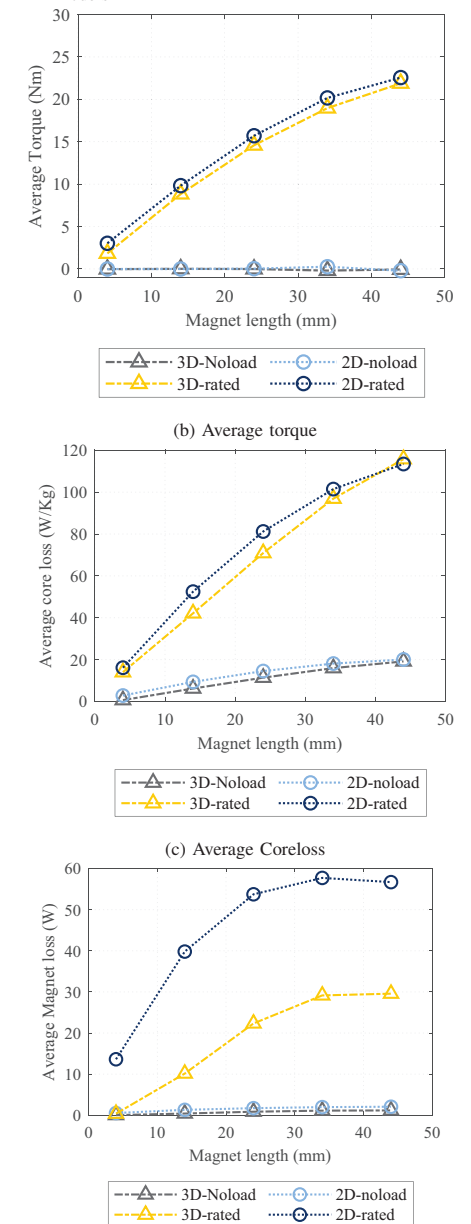
#### B. No-Load Test Analysis

At no-load when the machine is operated at rated speed 2000 rpm, the magnitude of flux linkages are studied for the five different models presented in Fig. 7. The flux linkage magnitude provides information about the leakage flux. It can be observed that models 1 and 2 have the lowest flux linkage with more leakage flux as compared to the other models. For a narrow core geometry, the winding end part is wider than the active part. The wider end winding part (in model 1) together

<sup>&</sup>lt;sup>b</sup>active part alone in the 2D model in radial direction



(a) Magnitude of flux linkages and percentage difference in the magnitude of flux linkage between the 3D and the 2D models



(d) Average Magnet loss
Fig. 5. Comparison of magnitude of flux linkages, average torque, average core loss and average magnet loss between 3D and the 2D models for varying core length and magnet length but plotted concerning magnet length for no-load and rated operation of the machine.

TABLE V
DESCRIPTION AND DIFFERENCES IN SELECTED MODELS

Model	Stator and Rotor Core length [mm]	Magnet length [mm]	Geometry modification in radial direction
Model 1 <sup>d</sup>	$6^c$	4	End winding and rotor core present
Model 2	6	4	End winding removed and rotor core present
Model 3	4	4	End winding present and rotor core removed
Model 4	4	4	End winding and rotor core absent
Model 5 <sup>e</sup>	4	4	End winding and rotor core absent

<sup>&</sup>lt;sup>c</sup>Applies only for Stator core

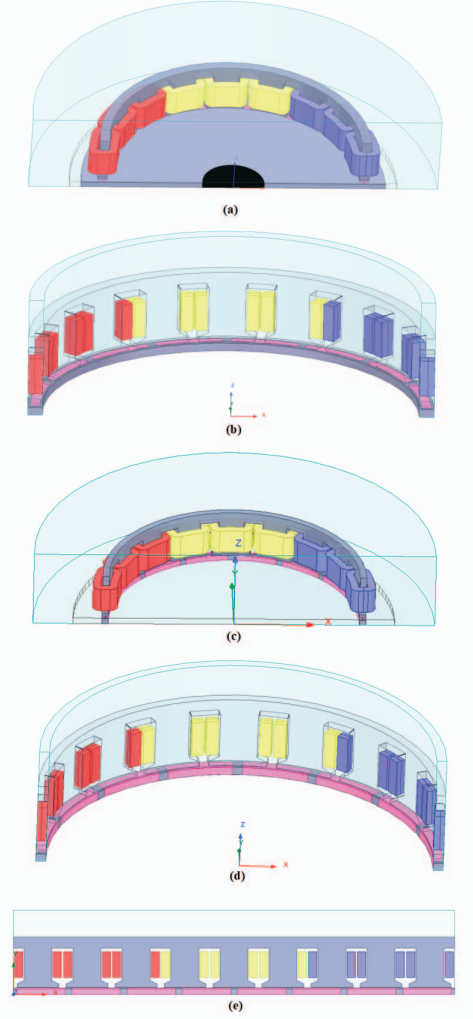


Fig. 6. Selected machine models to investigate the difference between the 3D and 2D model. (a) Model 1 - 3D model with end winding, magnet length = 4mm, core length = 6mm; (b) Model 2 - 3D model without end winding, magnet length = 4mm, stator and rotor core length = 6mm, (c) Model 3 - 3D model with end winding, magnet, stator and rotor core length = 4mm; (d) Model 4 - 3D model without end winding, magnet, stator core and rotor core length = 4mm; (e) Model 5 - 2D model with depth = 4mm

<sup>&</sup>lt;sup>d</sup>Full 3D model

e2D model

with the rotor core around the magnets (in models 1 and 2) account for a relatively higher end winding and magnet leakage flux.

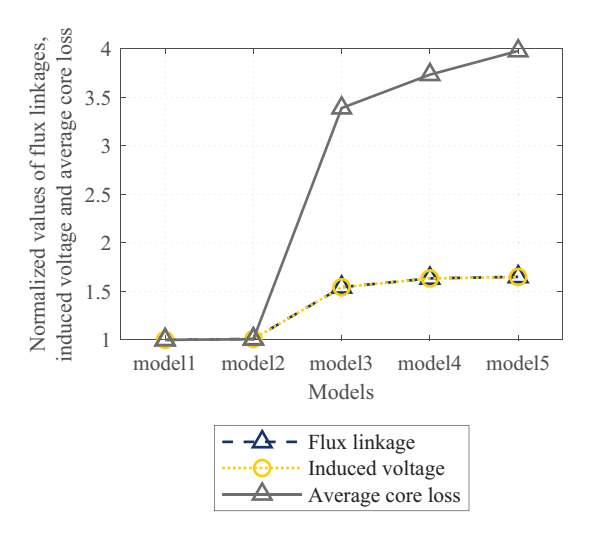


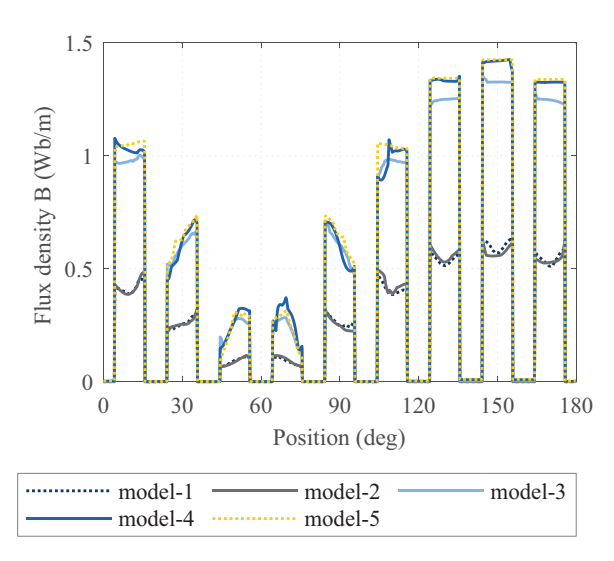
Fig. 7. Normalized values of the magnitude of flux linkage and induced voltage, average core loss at no-load for the five models

The normalized values of core loss follow the flux linkage values since the core loss depends on the square of the flux density. The flux density predicted by different models varies in the tooth as illustrated in Fig. 8a. The flux leakage from coils and magnets is illustrated in Fig. 8b. The illustration makes it apparent that the increased leakage flux in models 1 and 2 is attributable to the lower flux density in the teeth of models 1 and 2. The similar results of model 1 (with end windings) and model 2 (without end windings) clarify that the primary source of leakage flux is attributed to magnet flux leaking to the rotor core, with a lesser contribution from the end part of the winding. Likewise, the flux in models 1 and 2, with the rotor core positioned both outside and inside of the magnets, and without outside and inside rotor cores in models 3, 4, and 5, exhibits a more noticeable and substantial difference.

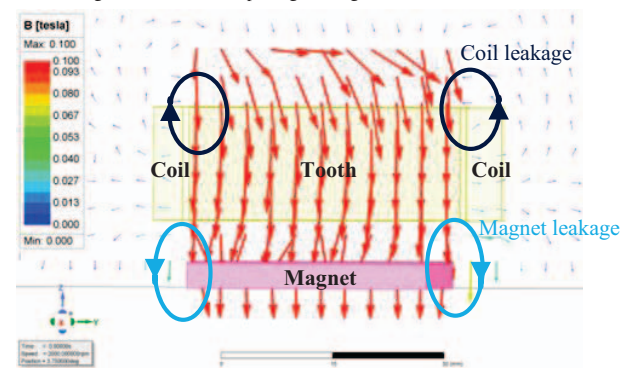
Cogging torque, core loss, and magnet loss are sensitive to selected mesh element size and number of time steps. In the models, a fine mesh is chosen, utilizing tetrahedral elements for the 3D model and triangular elements for the 2D model, with 120 time steps per period. However, cogging torque is especially sensitive, and before presenting results of torque ripple, even better discretization (in 3D) is required. Still, initial results of cogging torque in the five models show that the highest torque ripple is found in model 4. The boundary of model 4 lies along the core, and all magnet flux is recorded passing along the sharp corners of the teeth, hence larger torque ripples are to be expected.

#### C. Load Test Analysis

The load test analysis assesses the load torque and losses. The results in this section are recorded when the machine was



(a) Tooth flux density versus position (circumferentially) for half of the machine with 8 magnets and 9 slots depicting 180deg



(b) Flux density vectors in coils and magnets in the 3D FEM model Fig. 8. Flux density in parts of the machine

operated at 2000 rpm, with a maximum excitation current of 60A.

#### 1) Torque Analysis

The average torque concerning the load current is illustrated in Fig. 9. The average torque tends to saturate in models 1 and 3. Since models 1 and 3 encompass the end region with an end winding, the leakage flux around the end winding plays a role in the saturation of the stator core, with more flux leakage at higher currents. Models 2, 4, and 5 have boundary conditions that prevent the inclusion of this effect. Thus in subsequent models, all the currents are utilized effectively, and the flux remains contained within the active part of the machine.

#### 2) Core Loss Analysis

The core loss is illustrated in Fig. 10. In models 1 and 2 the leakage flux in the rotor core around the magnets and in the end part of the winding leads to a lower magnetic flux density in the tooth, similar to the no-load test. Consequently, the core loss is lower than in the other models at lower load currents. At high currents, the end winding leakage in model 1 induces increased core loss compared to model 2. A similar effect is observed in model 3, indicating a core loss

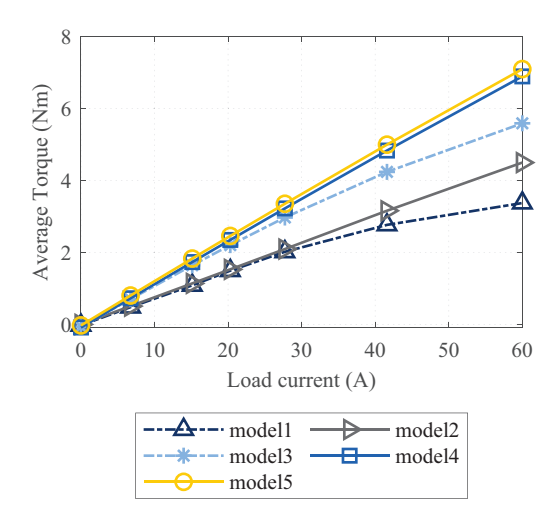


Fig. 9. Average torque of the five models; models 2, 4, and 5 depict a linearly increasing curve without the end parts of the winding; models 1 and 3 with the end part of the winding depict a slightly bent curve starting at 27A.

increase with increased currents. In models 2, 4, and 5 the core loss practically remains constant with increasing load current. Models 4 and 5 exhibit a minor difference in the average core loss, possibly attributable to the magnet skewing and the difference in mesh elements.

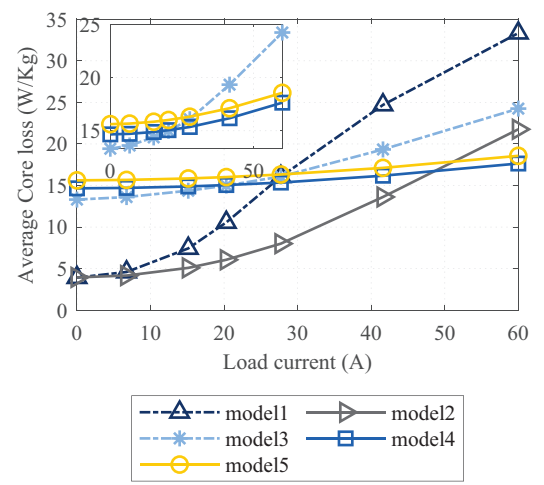


Fig. 10. Average core losses versus load current; the curves for models 3, 4, and 5 are zoomed in as they appear flat when plotted along models 1 and 2.

#### 3) Magnet Loss Analysis

Magnets play a crucial role in electrical machines and hence it is imperative to analyze the energy loss within the magnets. From the magnet loss plot illustrated in Fig. 11, it is seen that an increase in current leads to increased magnet loss in all models with the highest loss in models 4 and 5. The boundary condition in both models 4 and 5 forbids any leakage and hence the stator flux is channelized into the magnets. The steady increase in flux with an increase in load current induces circulating current within the magnets and hence the magnet losses are found to be greater in model 5. Nevertheless, it is the same with model 4 but the shape of the magnets is

trapezoidal as compared to the rectangular magnets in the 2D model (model 5). The lower magnet loss in model 4 compared to model 5 is due to the shape of the magnets and the different mesh elements. In contrast to models 4 and 5, models 1, 2, and 3 include the effects of leakage flux, resulting in lower magnet loss.

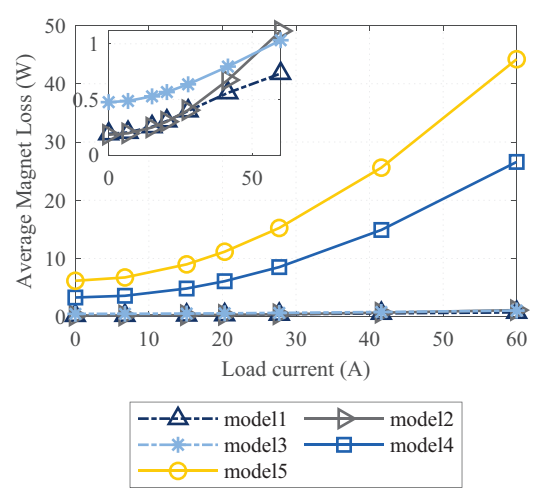


Fig. 11. Average magnet loss versus load current; Models 1, 2, and 3 are nearly flat and equal to zero in the main plot hence, the zoomed-in plots of these three models depict that the losses are low and increasing

#### 4) Copper Loss Analysis

The cross-section area of the copper is equivalent in all five models. However, in the 3D models, the volume of the copper in the winding is not the same when compared to the 2D model. The copper loss is illustrated in Fig.12. Model 1 and Model 3 have slight differences, although they both contain end windings. The stator core length is 6mm in model 1 (similar to model 2) and 4mm in model 3. As a consequence, there is a difference of 2mm in the active length of the coil. The copper loss in models 4 and 5 are the same as the models are geometrically equivalent regarding coil volume. The analysis of copper losses only includes DC copper loss, and examination of AC copper losses is beyond the scope of this paper.

#### V. CONCLUSION

The main purpose of this work is to investigate the differences between the 3D and 2D AFM models to provide accurate advice for when the quicker 2D modeling can provide adequate results. In contrast to RFMs, AFMs are much more dependent on 3D analysis. The AFPM machine is modeled in 3D FEM and the results are compared with measurements of an off-the-shelf reference AFM. The transformation of the 3D and 2D model was executed with a single computational plane located at a radius of  $R_{wp}=65.1mm$  traversing the center of the magnets with a radial thickness of  $L_m=34mm$  in the 3D model. The no-load flux linkages for varying core and magnet lengths were compared for the 3D and 2D AFM models. The model with narrow core and magnet lengths was further investigated and potential reasons aiding the leakage flux were analyzed. From the no-load and load-test data, we can

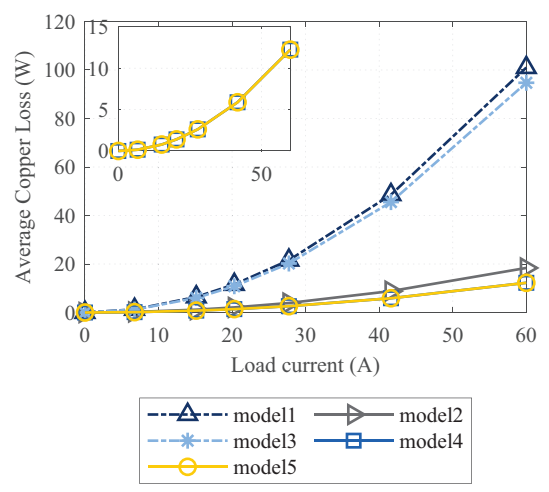


Fig. 12. Copper loss versus load current; models 4 and 5 have the same cross-section area and the depth of stator core; Models 1 and 3 have end part of the winding and the stator core length has a difference of 2mm; Model 2 is without the end part of the winding but with stator core length of 6mm.

conclude that the 3D AFMs with a wider core in the xy-plane can be transformed to an equivalent 2D model but the AFM with the narrow core is not feasible for transformation. For the investigated machine, the recommended ratio of magnet thickness in the radial direction is above 0.5, with a ratio of  $\frac{L_m}{R_{wp}} > 0.5$ . A 2D model can be used to simulate flux linkage, torque, and core and magnet loss, with the 2D computation plane at the radius  $R_{wp}$ . Still, the copper loss must be corrected to include the end winding copper loss. Suggested future work include considerations of AC copper loss and a comparison over the full torque speed range.

#### ACKNOWLEDGMENT

The authors acknowledge and extend gratitude to Xiaoliang Huang for his unwavering support in capturing the measurements.

#### REFERENCES

- [1] Solmaz Kahourzade et al. "Line-Start axial-flux PM motors: Introduction of a new machine topology". In: 2019 IEEE energy conversion congress and exposition (ECCE). IEEE. 2019, pp. 7027–7034.
- [2] F.N.U. Nishanth et al. "Design of an axial flux machine with an integrated hydraulic pump for off-highway vehicle electrification". In: 2020 IEEE Energy Conversion Congress and Exposition (ECCE). IEEE. 2020, pp. 1772–1779.
- [3] Hongwei Lan and Na Wang. "An Improved Quick Design for Axial Flux Permanent Magnet Synchronous Machine". In: 2023 7th International Conference on Smart Grid and Smart Cities (ICSGSC). IEEE. 2023, pp. 267–272.
- [4] Abdenour Abdelli et al. "Combination of 2D and 3D Finite Element Models in the Design of Axial Flux Permanent Magnet Machines for Electric Vehicle Applications". In: 2023 IEEE Workshop on Electrical

- *Machines Design, Control and Diagnosis (WEMDCD).* IEEE. 2023, pp. 1–6.
- [5] Haidar Diab, Yacine Amara, and Georges Barakat. "End-Effects Modeling in an Axial Field Flux Focusing Magnetic Gear using a Quasi-3D Reluctance Network Model". In: 2022 International Conference on Electrical Machines (ICEM). IEEE. 2022, pp. 83–88.
- [6] Aritz Egea et al. "Axial-flux-machine modeling with the combination of FEM-2-D and analytical tools". In: *IEEE transactions on industry applications* 48.4 (2012), pp. 1318–1326.
- [7] Mehmet Gulec and Metin Aydin. "Implementation of different 2D finite element modelling approaches in axial flux permanent magnet disc machines". In: *IET Electric Power Applications* 12.2 (2018), pp. 195–202.
- [8] Mustafa Özsoy, Orhan Kaplan, and Mehmet Akar. "Implementation of Different 2D Finite Element Modeling Approaches in Axial Flux Induction Motors". In: *Electric Power Components and Systems* 51.19 (2023), pp. 2385–2396.
- [9] Ahmed Shoeb and Sainan Xue. "Topology Optimization of Axial Flux Machines with a Simplified 2D Finite Element Approximation". In: 2023 IEEE Energy Conversion Congress and Exposition (ECCE). IEEE. 2023, pp. 4292–4296.
- [10] Jin Seok Kim et al. "Characteristics analysis method of axial flux permanent magnet motor based on 2-D finite element analysis". In: *IEEE Transactions on Magnetics* 53.6 (2017), pp. 1–4.
- [11] A Egea et al. "Axial flux machines modelling with the combination of 2D FEM and analytic tools". In: *The XIX International Conference on Electrical Machines-ICEM 2010*. IEEE. 2010, pp. 1–6.

#### **BIOGRAPHIES**

Vineetha Puttaraj is currently a PhD student at the Division of Electrical Power Engineering within the Department of Electrical Engineering at Chalmers University of Technology, Gothenburg, Sweden, specializing in the design of electrical machines, her research focuses on design analysis and testing of axial flux machines for vehicle applications. She earned her Master's degree in Computer application for Industrial Drives from Visveshwaraya Technological University, India. Her research interests are in the areas of electrical machines and drives.

Sonja Tidblad Lundmark was born in Gävle, Sweden, in 1966. She received her M.Sc. (Eng.) and Ph.D. degrees from Chalmers University of Technology, Gothenburg, Sweden, in 1992 and 2005, respectively. Since July 2013, she has been an Associate Professor at the Division of Electric Power Engineering at Chalmers University of Technology. Her research interests are in the areas of electrical machines and drives.

**Torbjörn Thiringer** works at Chalmers University of Technology, in Göteborg Sweden, as a professor in applied power electronics. He took his M.Sc and Ph.D at Chalmers University of Technology in 1989 and 1996 respectively. His areas of interest include the modeling, control and grid integration of wind energy converters into power grids, battery technology from detailed cell modelling to system aspects, as well as power electronics and drives for other types of applications, such as electrified vehicles, buildings and industrial applications.